<Original Paper> Journal of the Korean Society for Nondestructive Testing, Vol. 35, No. 6: 407-413, 2015
ISSN 1225-7842 / eISSN 2287-402X http://dx.doi.org/10.7779/JKSNT.2015.35.6.407

A Method to Simulate Frictional Heating at Defects in Ultrasonic Infrared Thermography

Wonjae Choi*†, Manyong Choi* and Jeonghak Park*

Abstract Ultrasonic infrared thermography is an active thermography methods. In this method, mechanical energy is introduced to a structure, it is converted into heat energy at the defects, and an infrared camera detects the heat for inspection. The heat generation mechanisms are dependent on many factors such as structure characteristics, defect type, excitation method and contact condition, which make it difficult to predict heat distribution in ultrasonic infrared thermography. In this paper, a method to simulate frictional heating, known to be one of the main heat generation mechanisms at the closed defects in metal structures, is proposed for ultrasonic infrared thermography. This method uses linear vibration analysis results without considering the contact boundary condition at the defect so that it is intuitive and simple to implement. Its advantages and disadvantages are also discussed. The simulation results show good agreement with the modal analysis and experiment result.

Keywords: Ultrasonic Infrared Thermography(UIRT), Frictional Heating, Defect, Simulation, Modelling

1. Introduction

Thermography is a method to detect defect on a structure using infrared(IR) camera. There are mainly two types: passive and active thermography [1]. “Active” means that external energy is applied to a target structure, which can be optical, electrical or mechanical, but “passive” method requires no external source. The active thermography gathers its importance in a variety of NDE fields [2,3], for example, composites [4] and dissimilar metal weld inspections [5]. Ultrasonic infrared thermography (UIRT) is one of the active methods and uses mechanical vibration as the energy source. It has been increasingly investigated as an NDE method since UIRT shows its potential to detect defects in complex structures, which are difficult to detect using conventional NDE method [5]. In addition, due to the rapid development in manufacturing, data processing capabilities, IR camera becomes less expensive than before and thus the method has been widening its application fields. However, it still needs more in-depth investigation and optimization to increase its stability.

In UIRT, mechanical energy is introduced to a structure in order to generate heat at target, and IR camera detects the heat for inspection. It has been known that there are several heat generation mechanisms such as friction, thermos-elastic effect, and plastic deformation [6].

However, it is difficult to predict how much heat is generated from each of the mechanisms, since it is dependent on many factors such as material and geometry of the structure inspected and excitation method. In experiments, it is difficult to control such factors accurately and independently. Thus, it would be very useful if the UIRT can be modelled and then virtually tested with the model to estimate its performance.

Modelling UIRT has been an issue to achieve its robust and stable estimation for heat distribution and been investigated during the

[Received: October 2, 2015, Revised: October 28, 2015, Accepted: October 29, 2015] *Center for Safety Measurement, KRISS, Daejeon 34113, Korea †Corresponding Author: w.choi@kriss.re.kr

past decades [7,8]. Numerical calculation using Finite Element Method (FEM), for example, has often been used to simulate all or part of the UIRT. One of the difficulties in the simulation is the fact that the heat mechanism is involved with physical contact of the two surfaces of a crack. This inevitably introduces nonlinearity to the simulation, and then the FEM computation becomes laborious. In this paper, a model to estimate frictional power is proposed without considering contact mechanism. Background theory will be introduced in the next section, and the proposed simulation procedure is explained in Section 3. A simulation results are described and analyzed in Section 4, and the results are compared with an experiment in Section 5. The paper is concluded in Section 6.

2. Heat Generation Mechanism in Vibro-Thermography

A typical UIRT setting is shown in Fig. 1. Heat is generated at crack, and IR camera detects the heat for inspection. In UIRT, there are several heat generation mechanisms such as friction, thermoelasticity and plastic deformation [6]. Frictional heating is known to be a main contributor to the heat generation at defect in a metal structure [9,10], and the mechanism is of interest in this paper.

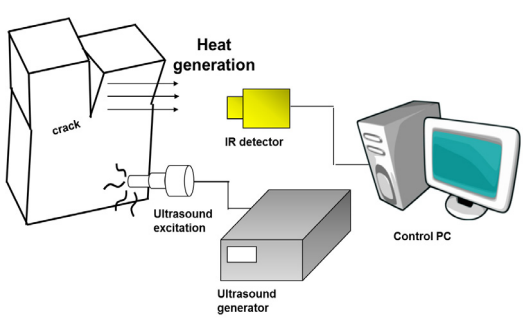

Fig. 1 Schematic of UIRT

Friction at a crack is created by contact between two crack faces. There are three vibration modes for crack [11] as in Fig. 2. The first mode shows clapping motion, and heat can be generated by volume deformation of the two side of the crack. In the other two modes, rubbing interaction creates frictional heat. The frictional power P at the contact area is known as a function of the relative force and velocity of the crack surfaces [12], which can be expressed as

$$P = \mu N v \tag{1}$$

where μ is friction coefficient, N is normal force, and v is tangential velocity as indicated in Fig. 3. Intheory, if the three factors in the right hand sides of Eq. (1) are known, the frictional power can be obtained. They maybe able to be estimated from computer simulations by appropriate model for the frictional behavior.

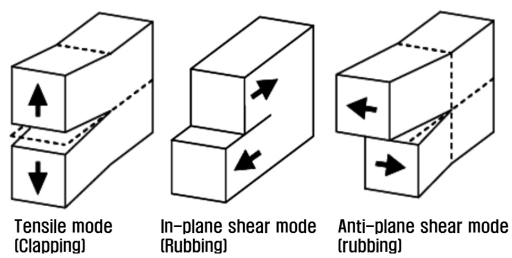

Fig. 2 Model for crack vibration modes from [11]

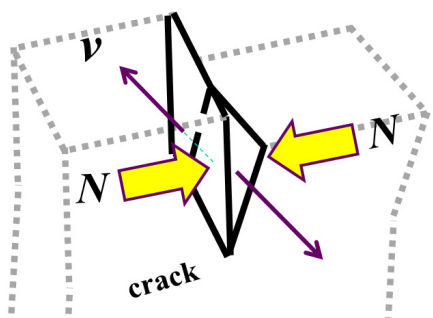

Fig. 3 Normal force and tangential velocity at a crack

3. Frictional Power Estimation at Defects

In order to estimate the frictional power, a method is proposed in this section. In this method, vibration analysis is first executed without considering a boundary condition at a defect, and then the power is estimated based on the motion of the crack surfaces. An example procedure is as follows. First, a model having a crack with zero width is created, in which all nodes have their pair and each pair is at the same location in the three dimensional space. Secondly, FEM is conducted to estimate vibration of motion of the crack surfaces with no contact boundary condition at the crack. Excitation to the model in this simulation can be harmonic or time series input. Once the simulation is completed, the displacement at the two crack surfaces is obtained from the FEM results. Note that since there is no contact condition, the two crack surfaces can be overlapped to each other, which cannot occur in real world. For each node pair, we can measure relative normal distance between the two. If the distance is negative, then the nodes are overlapped in the simulation as Fig. 4 (c) but we assume that contact occurs at the middle point of the pair hypothetically as in Fig. 4(d). Normal force N loaded at the node pair can be estimated proportional to half the relative normal distance $\triangle d_n$ as in Fig. 4(d), which can be described as

$$N \propto Y \triangle d_n / \triangle x \tag{2}$$

where Y is Young's modulus. Similarly, relative tangential distance $\triangle d_t$ can be found as in Fig. 4(b), and used for estimating tangential velocity v:

$$\nu \propto \triangle d_t / \triangle t \tag{3}$$

Then, the frictional power from Eq. (1) becomes

$$P \approx \mu E \frac{\triangle d_n}{\triangle x} \frac{\triangle d_t}{\triangle t} \tag{4}$$

The total friction energy E over the crack for a certain amount of time T can be calculated by integrating the power over the hypothetical contact area A and the given time T:

$$E = \int_T \int_A P \, dx dt \tag{5}$$

Since this procedure requires no contact boundary condition which leads to nonlinearity, it needs only a simulation tool for linear vibration analysis and thus is simple to implement. However, achieving the simplicity, the method scarifies a few realistic features. It is assumed that the element size is small enough to determine area of contact based on the relative location of the pair on the area, and the relative displacement $\triangle d_n$ and $\triangle d_t$ is large enough to generate frictional heat. There is no resistance between the crack surfaces during their vibration, which means that the friction power calculated by this method is the maximum possible power at the crack.

Nevertheless, the frictional power can be calculated based on the vibration motion of the crack, which is the main cause of the power, and the heat distribution estimated by this

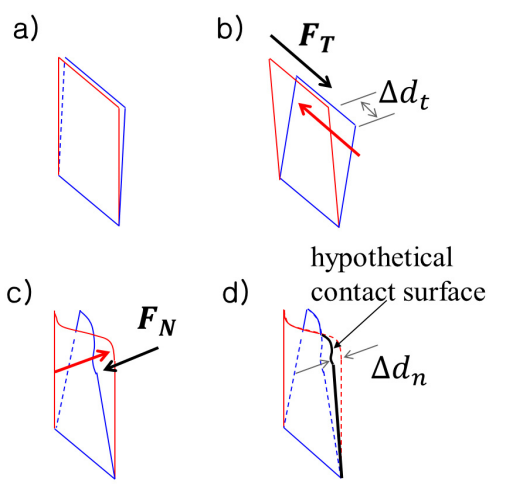

Fig. 4 Normal force and tangential velocity from the motion of crack surfaces for frictional power calculation

method can be used for qualitative comparison. It is useful to see the relative heat profile on the crack and to compare cases under different test environments. Using this method, friction power across crack area can readily be estimated and one example will be described in the next section.

4. Simulation

4.1. Frictional Power Estimation

The frictional power estimation is demonstrated in this section for a compact tensile (CT) specimen model as an example. It is 60 × 62 × 13 mm in size and has a 15 mm smooth crack as in Fig. 5. The material properties are shown in Table 1. The model was discretized approximately by 1 mm which corresponds to 1/75 of shear wavelength for 40 kHz excitation in the material and then it has approximately 145000 degree of freedom (DOF). The vibration analysis was conducted in time domain using explicit FEM code, Pogo [13]. Input to the specimen was simulated by uniform force given to nodes on a circular area of radius 5 mm in the specimen. Input frequencies are selected as 20, 30 and 40 kHz and the duration was 50 cycles. Note that the crack has zero width so that one node pair exists at one point on the crack area. Fig. 6 shows a cycle of vibration motion of the two crack surfaces.

As explained in the previous section, the two surfaces are freely overlapped to each other since there is no contact boundary condition. Based on the vibration displacement at the crack surfaces, hypothetical contact surface can be defined as in Fig. 4, and the frictional energy can then be estimated by Eqs. (2-5). The friction energies for 20, 30 and 40 kHz across the crack surface are in Fig. 7. The energy profiles for the all three frequencies have their maximum at the end (0 mm) and minimum at the tip of the crack (15 mm). This is reasonable since there is no rubbing at the tip and the crack surfaces have more freedom to move at

Table 1 Material properties of aluminum

	Young's modulus (GPa)	Density (kg/m^3)	Poisson ratio
Aluminum	700	2700	0.35

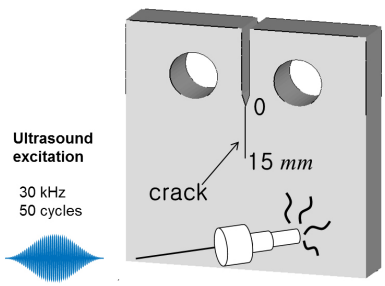

Fig. 5 CT sample for the simulation

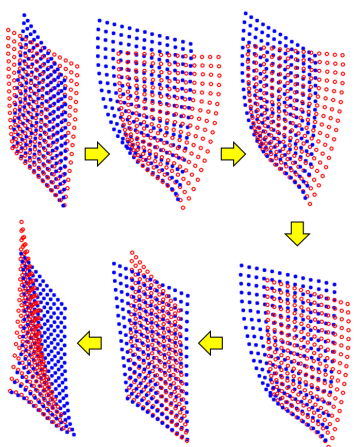

Fig. 6 One cycle of the two crack surfaces with 30 kHz excitation

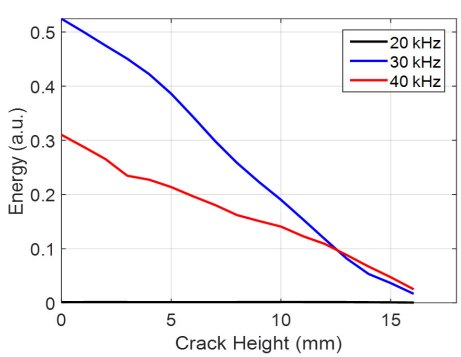

Fig. 7 Frictional energy across crack height for 20, 30 and 40 kHz excitation

the end. Interesting features of the graph are that it gets more energy with 30 kHz than 20 or 40 kHz excitation and it is virtually zero energy at 20 kHz. This is related to the motion of the crack. Fig 6 shows that the two surfaces are moving as they are rubbing each other (similar to the third mode in Fig. 2) so that the friction energy is higher than the other two results. This point can be explained more by its dominant motion of the crack surfaces, which will be explained in the next section.

4.2. Modal Analysis

In this section, modal analysis of the specimen was executed with a FEM open source, Calculix [14], for the FEM simulation. The discretized CT specimen model is the same as the one used in the previous section. Frequency range of interest was selected between 5 to 45 kHz, and 18 modes were found in total as shown in Fig. 8. Mode shapes of three modes are selected to see their vibration motion in Fig. 9, whose modal frequencies are closest to 20, 30, and 40 kHz.

Fig. 9 shows the three modes at opposite phase. For the 40 kHz case, the two crack surfaces are moving opposite in $\pm y$ direction as can be seen in Fig. 9(c). This motion corresponds to the second mode in Fig. 2. For 30 kHz case, the two surfaces are rubbing in $\pm x$ direction as in Fig. 9(b), corresponding to

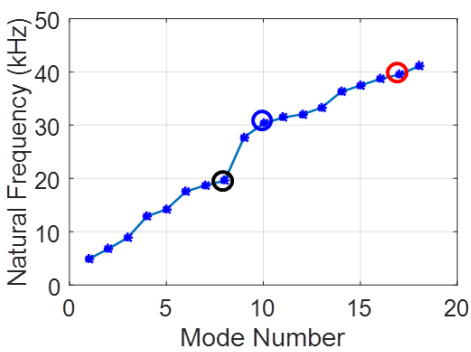

Fig. 8 Natural frequencies of the CT specimen

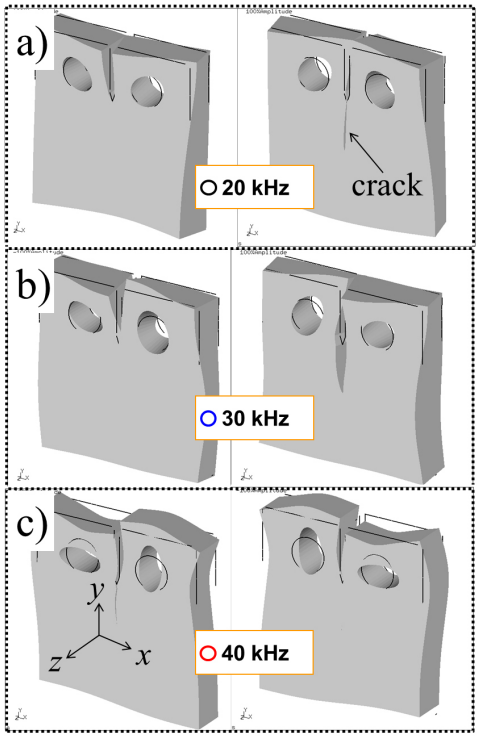

Fig. 9 Mode shapes for 20, 30 and 40 kHz

the third mode in Fig. 2. However, at 20 kHz, the two surfaces are moving in the same direction along z axis in Fig. 9(a), which generates virtually no friction at the crack. The results show that the rubbing mechanism at the vibration modes is responsible for the large frictional energy at 30 and 40 kHz in Fig. 7.

5. Comparison with an Experiment

The simulation result in the previous section is compared with an experimental result. The authors were conducted a vibrothermogrphy experiment in [10], and the result is used for the comparison. For completeness of the paper, short summary of the experiment is introduced here but for details see [10]. It was conducted with a CT sample which includes a microcrack as shown in Fig. 10. Size of the crack is approximately 11 mm and its width was measured as 10.9 micrometer at the end of the

crack and 2.1 micrometer at the tip of the crack. An ultrasonic excitation was given to the specimen and its frequency is 30 kHz.

Considering the crack width and temperature profile on the crack, the heating mechanism was concluded to be frictional heating in the reference. Fig. 10 shows an thermographic image after the specimen was excited. The temperature profile along the crack is indicated in Fig. 11 showing high temperature at the initiating point of the crack and low at the tip. The experimental result agrees well with the simulation one in Section 4 as can be seen in the figure. This is a qualitative comparison only for 30 kHz excitation case between the experiment and the simulation, but shows very promising results. More validation cases will be covered in future work to examine the usefulness of the frictional heating model.

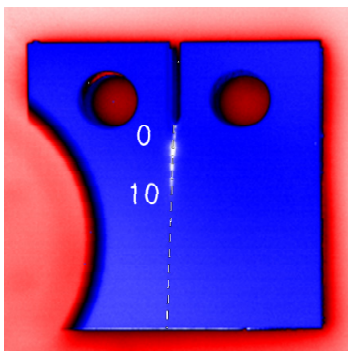

Fig. 10 Heat detected at the crack[9]

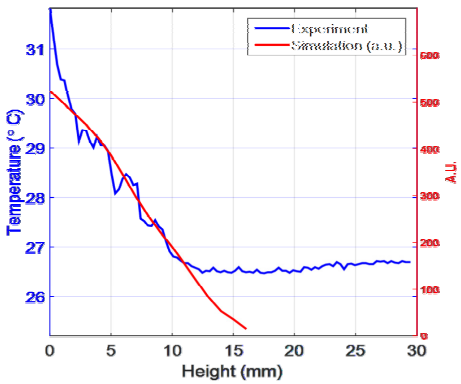

Fig. 11 Temperature profile along the crack from the simulation and experiment

6. Conclusion

A method to estimate frictional power at defect has been developed for UIRT and described in this paper, which uses a linear vibration model without considering contact boundary conditions at defects. Because of the linearity, this method is intuitive and simple to implement, but the frictional energy computed by the method may include quantitative margin due to the absence of contact effect. Nevertheless, it can be used to qualitatively estimate frictional energy based on the motion of the crack surfaces, which can be used for prediction of experiment results and parametric studies for UIRT.

Simulation using the method were conducted for a CT specimen with different excitation frequencies, and the results are compared well with modal vibration analysis results. The simulation result was also compared with an experiment and the temperature profile shows good agreement.

Acknowledgment

This work was supported by Radiation Technology R&D Program through the National Research Foundation of Korea funded by the Ministry of Science, ICT & Future Planning (No. NRF-2013M2A2A9043706) and by Nuclear Power Core Technology Development Program of the Korea Institute of Energy Technology Evaluation and Planning (KETEP) granted financial resource from the Korea Government Ministry of Knowledge Economy (No. 20121620100020).

References

[1] X. P. V. Maldague, "Theory and Practice of Infrared Technology for Nondestructive Testing," John Wiley & Sons, Inc. (2001)

[2] Y. Chung, S. Ranjit and W. Kim, “Thermal imaging for detection of SM45C subsurface defects using active infrared thermography techniques” *Journal of the Korean Society for Nondestructive Testing,* Vol. 35, No. 3, pp. 193-199 (2015)

[3] G. Kim, K. Lee, G. Kim, H. Hur, D. Kim and K. Chang, “Thermal resolution analysis of lock-in infrared microscope,” *Journal of the Korean Society for Nondestructive Testing,* Vol. 35, No. 1, pp. 12-17 (2015).

[4] K. Kwon, M. Choi, H. Park, J. Park, Y. Huh and W. Choi, "Quantitative defects detection in wind turbine blade using optical infrared thermography," *Journal of the Korean Society for Nondestructive Testing,* No. 35, No. 1, pp. 25-30 (2015)

[5] H. Park, M. Choi, J. Park and W. Kim, "A study on detection of micro-cracks in the dissimilar metal weld through ultrasound infrared thermography," *Infrared Physics & Technology*, Vol. 62, pp. 124-131 (2014)

[6] J. Renshaw, J. C. Chen, S. D. Holland and R. B. Thompson, "The sources of heat generation in vibrothermography," *NDT & E International*, Vol. 44, pp. 736-739 (2011)

[7] Z. Ouyang, L. D. Favro, R. L. Thomas and X. Han, "Theoretical modeling of thermosonic imaging of cracks," *Review of QNDE*, Vol. 21, AIP, 615, pp. 577-581 (2002)

[8] F. Mabrouki, M. Thomas, M. Genest and A. Fahr, "Frictional heating model for efficient use of vibrothermography," *NDT & E International*, Vol. 42, pp. 435-352 (2009)

[9] S. D. Holland, C. Uhl and J. Renshaw, "Vibrothermographic crack heating: a function of vibration and crack size," *Review of QNDE*, Vol. 28, AIP, 1096, pp. 489-494 (2009)

[10] M. Choi, S. Lee, J. Park, W. Kim and K. Kang, "Analysis of heat generation mechanism in ultrasound infrared thermography," *Journal of the Korean Society for Nondestructive Testing,* Vol. 29, No. 1, pp. 10-14 (2009)

[11] M. Rothenfusser and C. Homma, "Acoustic thermography: vibrational modes of cracks and the mechanism of heat generation," *Review of QNDE*, Vol. 24, AIP, 760, pp. 624-631 (2005)

[12] A. Saboktakin, C. Ibara-Castanedo, A. H. Bendada and X. Maldague, "Finite element analysis of heat generation in ultrasonic thermography," *Proceedings of QIRT*, pp. 619-624 (2010)

[13] P. Huthwaite, "Accelerated finite element elastodynamic simulations using the GPU," *J of Comp. Phys.*, Vol. 257, pp. 687-707 (2014)

[14] G. Dhondt and K. Wittig, Calculix, www.dhondt.de